Post-print of: Koziel S., Pietrenko-Dabrowska A., Leifsson L. (2019) Reduced-Cost Design Optimization of High-Frequency Structures Using Adaptive Jacobian Updates. In: Rodrigues J. et al. (eds) Computational Science – ICCS 2019. ICCS 2019. Lecture Notes in Computer Science, vol 11538. Springer, Cham
DOI: 10.1007/978-3-030-22744-9_40

Reduced-Cost Design Optimization of High-Frequency Structures Using Adaptive Jacobian Updates

Slawomir Koziel[1,2][0000-0002-9063-2647], Anna Pietrenko-Dabrowska[2][0000-0003-2319-6782], and Leifur Leifsson[3][0000-0001-5134-870X]

[1] Engineering Optimization & Modeling Center, School of Science and Engineering, Reykjavík University, Menntavegur 1, 101 Reykjavík, Iceland
koziel@ru.is
[2] Faculty of Electronics Telecommunications and Informatics, Gdansk University of Technology, Narutowicza 11/12, 80-233 Gdansk, Poland
annadabr1@pg.edu.pl
[3] Department of Aerospace Engineering, Iowa State University, Ames, IA 50011, USA
leifur@iastate.edu

Abstract. Electromagnetic (EM) analysis is the primary tool utilized in the design of high-frequency structures. In vast majority of cases, simpler models (e.g., equivalent networks or analytical ones) are either not available or lack accuracy: they can only be used to yield initial designs that need to be further tuned. Consequently, EM-driven adjustment of geometry and/or material parameters of microwave and antenna components is a necessary design stage. This, however, is a computationally expensive process, not only because of a considerable computational cost of high-fidelity EM analysis but also due to a typically large number of parameters that need to be adjusted. In particular, conventional numerical optimization routines (both local and global) may be prohibitively expensive. In this paper, a reduced-cost trust-region-based gradient search algorithm is proposed for the optimization of high-frequency components. Our methodology is based on a smart management of the system Jacobian enhancement which combines: (i) omission of (finite-differentiation-based) sensitivity updates for variables that exhibit small (relative) relocation in the directions of the corresponding coordinate system axes and (ii) selective utilization of a rank-one Broyden updating formula. Parameter selection for Broyden-based updating depends on the alignment between the direction of the latest design relocation and respective search space basis vectors. The proposed technique is demonstrated using a miniaturized coupler and an ultra-wideband antenna. In both cases, significant reduction of the number of EM simulations involved in the optimization process is achieved as compared to the benchmark algorithm (computational speedup of 60 percent on average). At the same time, degradation of the design quality is minor.

Keywords: Electromagnetic simulation, microwave engineering, antenna design, design optimization, gradient-based search, Jacobian update, trust region framework.

1 Introduction

Similarly as in many other engineering disciplines, design of high-frequency systems (e.g., microwave [1], antenna [2], photonic [3], etc.) is heavily based on computer simulation tools. While in some cases, analytical representations (e.g., array factor models for antenna array radiation patterns [4], or coupling-matrix-based models for microwave filters [5]) or equivalent network models (e.g., for transmission-line-based circuits [6]) are available, the ultimate level of accuracy and generality can be achieved by full-wave electromagnetic (EM) simulation [7]. As a matter of fact, EM analysis is mandatory for design verification of vast majority of contemporary high-frequency components and devices, which is due to their geometrical complexity. The latter is a consequence of more and more stringent performance requirements imposed on the components, demands for multi-band operation [8], additional functionalities (e.g., band notches in wideband antennas [9]), and, most importantly, compact size [10]-[13]. It is especially the miniaturization requirement that results in the development of topologically complex layouts exhibiting considerable EM cross-coupling effects, impossible to be adequately accounted for using analytical or equivalent circuit models. Examples include microwave components exploiting a slow-wave phenomenon [14] or defected ground structures [15], as well as compact antennas incorporating stepped-impedance feeds [16] or modified radiators [17].

Whenever electromagnetic simulation is involved, some variation of parametric optimization is necessary in order to obtain the best possible performance of the component at hand. Application of conventional numerical optimization methods, either local [18] or global [19], faces considerable challenges which come from several sources: (i) a high cost of individual EM analysis, (ii) a necessity of simultaneous handling of multiple performance figures and constraints, and (iii) a large number of simulations required to converge to the optimized design. The latter is partially due to the fact that geometries of modern high frequency structures are typically described by many parameters [20], [21]. All of these factors result in a considerable computational cost of the optimization process, often prohibitive. It should be mentioned here that a commonly used workaround these issues is an interactive design that combines engineering experience and parameter sweeping (one, maximum two parameters at a time). This is a laborious process yet incorporation of the expert knowledge permitted, in many cases, finding a satisfactory design relatively quickly. However, the aforementioned increase of component complexity, has made this approach questionable, especially in the context of controlling multiple objectives, handling constraints, and operating in highly-dimensional parameter spaces.

Meanwhile, several methods have been developed and applied to reduce the cost of numerical optimization. These include utilization of adjoint sensitivities (in the context of local design [22]), machine learning methods (for global optimization [23]), as well as various surrogate-assisted techniques [24]-[26]. The last group of approaches comes in many variations and involves both data-driven surrogates (e.g., kriging [27], Gaussian process regression [28], or polynomial response surfaces [29]), and physics-based ones. In the latter case, the surrogate is constructed from the underlying low-fidelity model (space mapping [30], response correction techniques [31], feature-based optimization [32]). For the sake of computational efficiency, the low-fidelity models should

be cheap (e.g., analytical or equivalent network ones). However, in many situations, e.g., antennas or various classes of miniaturized microwave components, the only reliable option for low-fidelity models are those obtained from coarse-discretization EM simulations [33]. Here, the overhead related to optimizing the surrogate model (often carried out using conventional algorithms) determines the overall design expense.

As discussed above, reducing the number of EM simulations required by an optimization routine is important for both direct and surrogate-assisted design procedures. In this paper, a low-cost trust-region-based gradient search algorithm is proposed for the optimization of high-frequency structures. The foundation of the method is an appropriate management of the system response sensitivity (here, Jacobian) updates. This management scheme involves a few mechanisms, including an omission of (finite-differentiation-based) sensitivity updates for variables that exhibit small (relative) relocation in the directions of the corresponding coordinate system axes as well as a selective application of a rank-one Broyden updating formula. The Broyden-based updates are performed for parameters whose corresponding basis vectors are sufficiently well aligned with the direction of the latest design relocation. For the sake of demonstration, two high-frequency structures are considered: a miniaturized coupler implemented using compact microstrip resonant cells (CMRCs), and an ultra-wideband antenna operating in 3.1 GHz to 10.6 GHz frequency range. In both cases, application of the proposed algorithm leads to a significant reduction of the number of EM simulations necessary for identifying the optimized design. The average computational speedup is as high as 60 percent as compared to the reference algorithm. The improvement of computational efficiency is achieved with only minor degradation of the design quality.

2 Reduced-Cost Design Optimization through Jacobian Update Management

In this section, the proposed procedure for expedited design optimization of high-frequency structures is formulated and explained. Here, local optimization is considered with the trust-region gradient search utilizing numerical derivatives used as a reference algorithm. The section starts by formulating the high-frequency design optimization problem, followed by a brief description of the reference algorithm, the proposed sensitivity updating scheme, as well as the complete optimization framework.

2.1 High-Frequency Design Problem Formulation

The computational model of the high-frequency structure of interest will be denoted as $\boldsymbol{R}(\boldsymbol{x})$, where $\boldsymbol{x}$ stands for the adjustable variables of the problem (typically, geometry parameters). $\boldsymbol{R}$ represents the model responses which are typically frequency characteristics such as scattering parameters (e.g., reflection S_{11}, transmission S_{21}, etc.), gain, efficiency, radiation pattern, power split ration, and so on. The computational model is assumed to be evaluated using a full-wave electromagnetic (EM) analysis. Normally, computational cost of EM simulation is considerable, ranging from a few dozens of seconds to a few hours, depending on the structure complexity, its electrical size (i.e., physical dimensions as compared to the guided wavelength at the operating frequency),

as well as other components that need to be included in the model (e.g., SMA connectors, housing, installation fixtures, etc.).

The design problem can be formulated as

$$\boldsymbol{x}^* = \arg\min_{\boldsymbol{x}} U\left(\boldsymbol{R}(\boldsymbol{x})\right) \tag{1}$$

where $\boldsymbol{x}^*$ is the optimum design to be found and U is a scalar objective function encoding the performance specifications imposed on the structure at hand.

Given a large variety of high-frequency structures and the figures of interest involved, it is obvious that the objective function is very much problem dependent. For the sake of illustration we will discuss two types of objective functions, pertinent to particular illustration cases considered in Section 3.

In many situations, especially related to the design of antenna structures but also certain other components such as impedance transformers or microwave filters, it is important to improve the in-band matching (which is equivalent to minimization of the reflection response S_{11} or reducing the return loss). In this case, the objective function may be defined as

$$U(\boldsymbol{R}(\boldsymbol{x})) = \max_{f \in F} |S_{11}(\boldsymbol{x}, f)| \tag{2}$$

where $|S_{11}(\boldsymbol{x},f)|$ stands for the reflection as a function of optimization variables $\boldsymbol{x}$ and frequency f, with F being the frequency range of interest (e.g., 3.1 GHz to 10.6 GHz in case of UWB antennas). The problem (1), (2) is thus formulated in a minimax sense.

The objective function (2) addresses a single performance figure. However, in majority of practical cases, there is a need to control several figures. Representative examples are microwave couplers, where a typical design problem requires maximization of the bandwidth BW (usually, symmetric with respect to the operating frequency f_0), obtaining the required (e.g., equal) power split $d_S = |S_{21}| - |S_{31}|$ at f_0, as well as the allocation of the matching and isolation characteristics ($|S_{11}|$ and $|S_{41}|$) minima close to f_0. In this case, assuming implicit constraint handling, we may define U as

$$U(\boldsymbol{R}(\boldsymbol{x})) = -BW(\boldsymbol{x}) + \sigma_1 d_S(\boldsymbol{x})^2 + \sigma_2 (f_{\min.S_{11}}(\boldsymbol{x}) - f_0)^2 + \sigma_3 (f_{\min.S_{41}}(\boldsymbol{x}) - f_0)^2 \tag{3}$$

where $f_{\min.S11}$ and $f_{\min.S41}$ are the frequencies corresponding to $|S_{11}|$ and $|S_{41}|$ minima, respectively, and σ_k are penalty coefficients. A penalty function approach as in (3) is a convenient way of handling expensive constraints, especially when dealing with EM simulation models [34], [35].

2.2 Trust-Region Gradient Search

The reference optimization algorithm for this paper is a conventional trust-region (TR)-based gradient-search procedure [18]. The TR algorithm yields a series of approximations $\boldsymbol{x}^{(i)}$, $i = 0, 1, \ldots$, to the optimum design $\boldsymbol{x}^*$, by solving sub-problems

$$\boldsymbol{x}^{(i+1)} = \arg\min_{\boldsymbol{x};\, -\boldsymbol{d}^{(i)} \le \boldsymbol{x} - \boldsymbol{x}^{(i)} \le \boldsymbol{d}^{(i)}} U(\boldsymbol{L}^{(i)}(\boldsymbol{x})) \tag{4}$$

In (4), $\boldsymbol{L}^{(i)}(\boldsymbol{x}) = \boldsymbol{R}(\boldsymbol{x}^{(i)}) + \boldsymbol{J}_{\boldsymbol{R}}(\boldsymbol{x}^{(i)})\cdot(\boldsymbol{x} - \boldsymbol{x}^{(i)})$ is a first-order Taylor expansion of the computational model $\boldsymbol{R}$ at the current iteration point $\boldsymbol{x}^{(i)}$. The Jacobian $\boldsymbol{J}_{\boldsymbol{R}}$ can be evaluated using adjoint sensitivities if available; however, in vast majority of practical cases of high-frequency structure design it is estimated through finite differentiation (FD). The reason is that the adjoint technology is not supported (with rare exceptions) by commercial EM simulation packages. FD incurs the cost of additional n EM analyses (n

being dimensionality of the design space) per algorithm iteration. Obviously, reducing this overhead would lead to computational savings, which is the main subject of this paper.

It should also be noticed that the trust region size in (4) does not take a traditional form of $\|\boldsymbol{x} - \boldsymbol{x}^{(i)}\| \leq \delta^{(i)}$ (Euclidean norm with scalar TR radius), but it is an interval defined through the size vector $\boldsymbol{d}^{(i)}$ (adjusted using the standard rules [18]). The inequalities $-\boldsymbol{d}^{(i)} \leq \boldsymbol{x} - \boldsymbol{x}^{(i)} \leq \boldsymbol{d}^{(i)}$ are understood component-wise. This type of the TR region allows—by making the initial size vector $\boldsymbol{d}^{(0)}$ proportional to the design space sizes—for ensuring a similar treatment of variables with significantly different ranges, a situation common in the antenna or microwave design. For example, the lengths of the transmission line components are typically in the range of millimeters or tens of millimeters, whereas the line widths or spacings between them may be small fractions of millimeters.

2.3 Reduced-Cost TR Algorithm Using Adaptive Jacobian Updates

The computational cost of the design optimization involving the conventional TR algorithm is primarily determined by the cost of Jacobian estimation performed using the finite differentiation. Here, a reduced-cost TR algorithm using adaptive Jacobian updates is introduced which allows us to notably decrease the number of EM simulations necessary to obtain the optimal design. The computational savings result from the reduction of the overall number of FD calculations. The algorithm combines two independent procedures for suppressing Jacobian updates: an accelerated update procedure (AUP) and Broyden update procedure (BUP). The former is based on a relative relocation of the design variable vector between iterations, and the optimization run history. The latter adopts the Broyden updating formula for the selected design variables, depending on the alignment between the most recent design relocation and the coordinate system axes. When used separately, each procedure allows for achieving considerable computational savings, however, at the expense of a slight degradation of the design quality, as shown in Section 3. Furthermore, a combination of both procedures further expedites the optimization process while ensuring satisfactory design quality. The essential stages of the proposed reduced-cost TR algorithm are shown in the form of a flow diagram in Fig. 1.

The information about either performing (1) or omitting (0) FD calculation of the system response Jacobian $\boldsymbol{J_R}$ is stored in a selection matrix $\boldsymbol{\Gamma}$. The complete description of the procedure of creating the matrix $\boldsymbol{\Gamma}$ is provided in Section 2.4., along with the account of the two component procedures: accelerated update procedure and Broyden update procedure. Here, the major outline of the modified TR algorithm is given. The selection matrix $\boldsymbol{\Gamma}$ is initialized as a column vector, $n \times 1$, with all its entries set to ones: $\gamma_{k.1} = 1$, $k = 1, \ldots, n$. This implies that in the first iteration, the initial estimate of the entire Jacobian $\boldsymbol{J_R}$ is obtained with FD. Upon each successful iteration, the matrix is extended by an additional column, utilized to govern the Jacobian update in the upcoming iteration (as depicted in Fig. 2).

After the Jacobian update is completed, a candidate design $\boldsymbol{x}_{tmp}$ is found by solving (4), with the objective function U described by (2) or (3). Then, a gain ratio $\rho =$

$(U(\boldsymbol{R}(\boldsymbol{x}_{tmp}) - U(\boldsymbol{R}(\boldsymbol{x}^{(i)})/(\boldsymbol{L}^{(i)}(\boldsymbol{x}_{tmp}) - \boldsymbol{L}^{(i)}(\boldsymbol{x}^{(i)}))$ is calculated, and the TR region size $\boldsymbol{d}^{(i+1)}$ for the next $(i+1)$th iteration is adjusted. If the gain ratio is positive, the candidate step is accepted and the next iteration is executed, unless the termination criterion is satisfied, i.e., $\|\boldsymbol{d}^{(i+1)}\| < \varepsilon$ and $\|\boldsymbol{x}^{(i+1)} - \boldsymbol{x}^{(i)}\| < \varepsilon$, where ε is the algorithm termination threshold.

2.4 Selection Matrix Updating Procedure

In this section, a procedure for updating the selection matrix $\boldsymbol{\Gamma}$ is described in detail. It combines two separate routines that control the Jacobian update: the accelerated (AUP) and the Broyden (BUP) update procedure. The former pinpoints the parameters that exhibit small relative design changes between iterations, therefore implying that the calculation of the respective part of the Jacobian can be omitted.

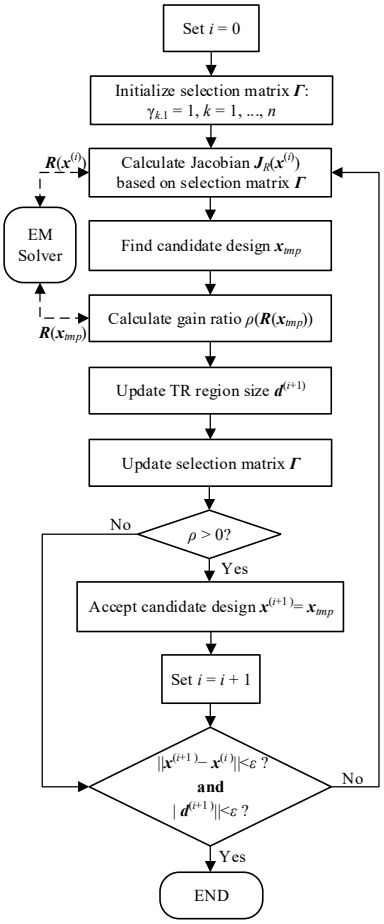

Fig. 1. Flow diagram of the proposed algorithm using adaptive sensitivity updating scheme. The following notation is used: $\boldsymbol{\Gamma}$ – selection matrix containing information about the Jacobian updates, $\boldsymbol{d}^{(i+1)}$ – TR region size in the $(i+1)$th iteration, ρ – gain ratio (deciding about iteration acceptance and $\boldsymbol{d}^{(i+1)}$ update), ε – algorithm termination threshold.

Whereas, the latter identifies the parameters for which the corresponding basis vectors are sufficiently well aligned with the most current design relocation vector. For these parameters, calculation of the respective Jacobian columns will be executed using the Broyden formula instead of FD. The outcomes of both procedures are then combined to create the selection matrix. The two procedures, along with the resulting Jacobian update procedure are presented in the form of a flow diagram in Fig. 2.

Accelerated Update Procedure. The accelerated procedure, depicted in Panel A of Fig. 2, accommodates the changes of geometry parameters observed throughout the optimization course. These are quantified by calculating a relative design change of the kth parameter, $k = 1, \ldots, n$, w.r.t. the TR region size in the ith iteration

$$\alpha_k^{(i+1)} = \left| x_k^{(i+1)} - x_k^{(i)} \right| \Big/ d_k^{(i)}, \qquad k = 1, \ldots, n, \tag{5}$$

where $x_k^{(i)}$, $x_k^{(i+1)}$ and $d_k^{(i)}$ refer to the kth components of vectors $\boldsymbol{x}^{(i)}$, $\boldsymbol{x}^{(i+1)}$, and $\boldsymbol{d}^{(i)}$, respectively. Let us also denote by $\boldsymbol{J}_k$ the kth column of the Jacobian $\boldsymbol{J}_R$. The decision factors $\alpha_k^{(i+1)}$ are utilized to determine whether $\boldsymbol{J}_k$, pertaining to the kth parameter of the structure at hand, is to be calculated using FD in the next, $(i+1)$th, iteration. Additionally, the optimization run history is inspected, in order to ensure that the part of the Jacobian $\boldsymbol{J}_k$ is computed at least once every few iterations.

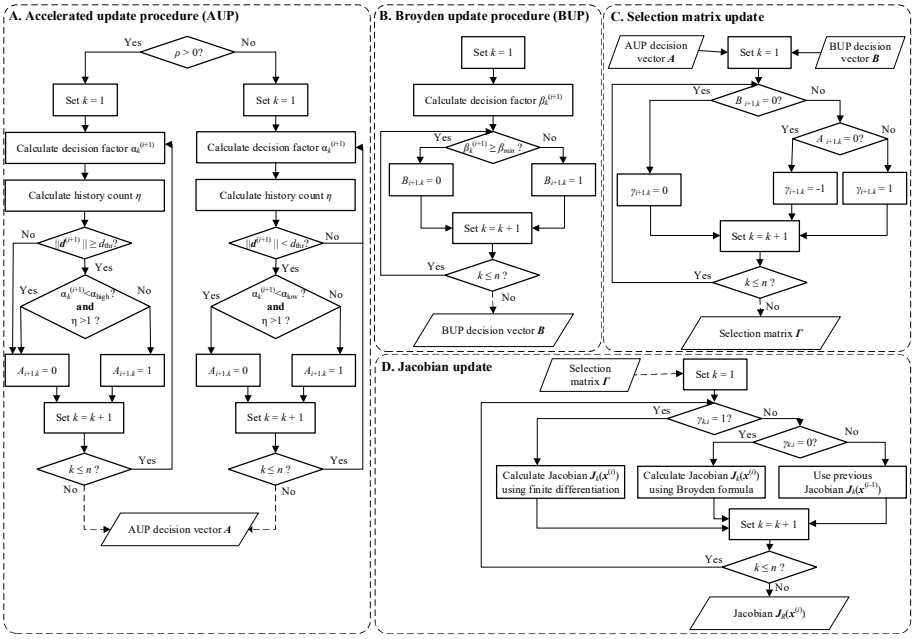

Fig. 2. Flow diagram of the selection matrix update procedure: A) accelerated update procedure, B) Broyden update procedure, C) selection matrix $\boldsymbol{\Gamma}$ update based on AUP and BUP, D) Jacobian update based on $\boldsymbol{\Gamma}$. The following notation is used: (i) AUP parameters: $\alpha_k^{(i+1)}$ – decision factor for kth geometry parameter and $(i+1)$th iteration; η – history count, α_{high}, α_{low} – threshold values, $\boldsymbol{A}$ – AUP decision vector; (ii) BUP parameters: $\beta_k^{(i+1)}$ – decision factor for kth geometry parameter and $(i+1)$th iteration, $\beta_{\min}$ – alignment threshold value, $\boldsymbol{B}$ – BUP decision vector.

The update history is examined in the course of the last N iterations (N being the algorithm control parameter), and a history count η is defined as a total number of iterations, among the last N iterations, in which the Jacobian update using FD was carried out. Both the decision factors $\alpha_k^{(i+1)}$ and the history count η are then translated into a binary AUP decision vector $\boldsymbol{A}$ that stores the information about the update for the upcoming iteration. Let us denote by $A_{i+1.k}$ the kth entry of the vector $\boldsymbol{A}$ referring to the (i+1)th iteration. If the entry of the vector $\boldsymbol{A}$ equals zero, i.e., $A_{i+1.k} = 0$, AUP indicates that, for the kth parameter of the structure at hand, the respective Jacobian column $\boldsymbol{J}_k$ does not have to be calculated with FD in the next iteration; otherwise, i.e., if $A_{i+1.k} = 1$, FD is suggested.

As shown in Fig. 2, at the beginning of AUP, a decision factor $\alpha_k^{(i+1)}$ (see (5)) and history count η are calculated for all parameters. Then, the entries of the decision vector $\boldsymbol{A}$ are established depending on whether the iteration was successful ($\rho > 0$) or not ($\rho \leq 0$). If the iteration was accepted, $A_{i+1.k}$ is set to 0 in the two following cases:

1. For all parameters, if the TR size in the next iteration $\|\boldsymbol{d}^{(i+1)}\|$ is small, below a user-specified threshold d_{thr},
2. For the selected parameters: if the TR region size in the next iteration $\|\boldsymbol{d}^{(i+1)}\|$ exceeds the threshold d_{thr}, and if, for a given parameter k, the Jacobian column $\boldsymbol{J}_k$ was: (i) calculated with FD at least once in the last N iterations and (ii) the factor $\alpha_k^{(i+1)}$ is below the user-specified threshold α_{high}.

In the case of the rejected iteration, (i.e., $\rho \leq 0$), as a rule, the decision vector established in the previous iteration, and stored in the selection matrix $\boldsymbol{\Gamma}$, is not altered. However, if $\|\boldsymbol{d}^{(i+1)}\|$ is below the threshold d_{thr}, $A_{i+1.k}$ is set to 0, when simultaneously the two following conditions are met: (i) $\alpha_k^{\,i} < \alpha_{\text{low}}$ and (ii) $\boldsymbol{J_k}$ was calculated with FD at least once in the last N iterations. The user defined thresholds fulfill the condition: $0 < \alpha_{\text{low}} < \alpha_{\text{high}} < 1$, in order to ensure more frequent updates, if the iteration was unsuccessful.

Broyden Update Procedure. Here, the Broyden update procedure, shown in Panel B of Fig. 2, is described in detail. During BUP, the parameters for which the alignment between the most recent design relocation and the coordinate system axes is satisfactory, are selected. Then, the corresponding columns of the circuit response Jacobian $\boldsymbol{J_R}$, are calculated using the Broyden formula (BF) instead of FD. Here, we adopt a rank-one Broyden update [36]

$$\boldsymbol{J_R}^{(i+1)} = \boldsymbol{J_R}^{(i)} + \frac{\left(\boldsymbol{f}^{(i+1)} - \boldsymbol{J_R}^{(i)} \cdot \boldsymbol{h}^{(i+1)}\right) \cdot \boldsymbol{h}^{(i+1)T}}{\boldsymbol{h}^{(i+1)T}\boldsymbol{h}^{(i+1)}}, \qquad i = 0, 1, \ldots \tag{6}$$

where the following notation is used: $\boldsymbol{f}^{(i+1)} = \boldsymbol{R}(\boldsymbol{x}^{(i+1)}) - \boldsymbol{R}(\boldsymbol{x}^{(i)})$, and $\boldsymbol{h}^{(i+1)} = \boldsymbol{x}^{(i+1)} - \boldsymbol{x}^{(i)}$. Note that (6) only updates the Jacobian in the one-dimensional subspace spanned by $\boldsymbol{h}^{(i)}$ and at least n executions of (6) are necessary to obtain $\boldsymbol{J_R}$ information within the entire space. Consequently, in higher-dimensional spaces, unsatisfactory results are usually obtained when the Jacobian is calculated solely using (6). Here, $\boldsymbol{J_R}$ updating involves both FD and BF.

Let us denote by $\boldsymbol{e}^{(k)}$ the standard basis vectors, i.e., $\boldsymbol{e}^{(k)} = [0 \ldots 0\ 1\ 0 \ldots 0]^T$ with 1 on the kth position. In the BUP procedure, for each parameter k, the values of the alignment factors $\beta_k^{(i+1)} = |\boldsymbol{h}^{(i+1)T}\boldsymbol{e}^{(k)}|/\|\boldsymbol{h}^{(i+1)}\|$ are calculated. The factors $\beta_k^{(i+1)}$ act as a quantification measure of the alignment between the current design relocation $\boldsymbol{h}^{(i+1)}$ and the respective basis vectors $\boldsymbol{e}^{(k)}$. Note that $0 \leq \beta_k^{(i+1)} \leq 1$ ($\beta_k^{(i+1)} = 0$ and $\beta_k^{(i+1)} = 1$, if $\boldsymbol{h}^{(i+1)}$ and $\boldsymbol{e}^{(k)}$ are

orthogonal and co-linear, respectively). For a given parameter k, the respective entry of the BUP decision vector $B_{i+1.k}$ is set to 0, if the alignment $\beta_k^{(i+1)}$ is better than a user-defined alignment acceptance threshold $\beta_{\min}$, otherwise $B_{i+1.k} = 1$; $\beta_{\min}$ is a control parameter for BUP: the higher $\beta_{\min}$, the more stringent the condition for using BF gets, which likely leads to lower computational savings but higher quality of the obtained solution.

Jacobian Update. Upon performing AUP and BUP, the selection matrix $\boldsymbol{\Gamma}$ is altered and the Jacobian update is performed accordingly. $\boldsymbol{\Gamma}$ is extended by adding the (i+1)th column after each successful iteration. The added column is computed from both AUP and BUP in the following manner (see Panel C of Fig. 2). For a given index k, the entry $\gamma_{i+1,k}$ is set to 0, if the $B_{i+1.k}$ equals 0 (disregarding the value of $A_{i+1.k}$). In that case, the respective Jacobian column $\boldsymbol{J}_k$ is estimated using BF. Otherwise, if $B_{i+1.k} = 1$ and $A_{i+1.k} = 0$, then $\gamma_{i+1,k}$ is set to –1 which indicates that the Jacobian from the previous iteration is to be used, i.e., $\boldsymbol{J}_k(\boldsymbol{x}^{(i+1)}) = \boldsymbol{J}_k(\boldsymbol{x}^{(i)})$. Finally, if $B_{i+1.k} = A_{i+1.k} = 1$, $\boldsymbol{J}_k$ is obtained using FD. Thus, FD is performed exclusively if both routines conclude it is mandatory. Consequently, substantial computational savings are secured, as it is confirmed by the results presented in Section 3. At the same time, the observed degradation of the solution quality is practically acceptable. The algorithmic flow of the Jacobian update procedure is shown in Panel D of Fig. 2.

3 Numerical Results and Benchmarking

Here, two high-frequency structures are considered as a benchmark set: an equal-split rat-race coupler (RRC) composed of compact microstrip resonant cells (CMRCs) [37] shown in Fig. 1(a), and a wideband antenna [38] (Fig. 1(b)). The first structure (RRC) is implemented on Taconic RF-35 substrate (h = 0.762 mm, ε_r = 3.5, tanδ = 0.0018). The RRC geometry is described by a parameter vector $\boldsymbol{x} = [w_1\ l_1\ w_2\ l_2\ w_3]^T$. Relative dimensions are $l_3 = 19w_1 + 18w_2 + w_3 - l_1$, $l_4 = 5w_1 + 6w_2 + l_2 + w_3$, $l_5 = 3w_1 + 4w_2$ and $w_4 = 9w_1 + 8w_2$ (all in mm). The coupler is supposed to operate at f_0 = 1 GHz and it has been optimized for maximum bandwidth (defined at –20 dB level of matching and isolation), and symmetric around f_0.

The antenna [37] is also implemented on RF-35 substrate, and it has the following independent geometry parameters $\boldsymbol{x} = [L_0\ dR\ R\ r_{rel}\ dL\ dw\ L_g\ L_1\ R_1\ dr\ c_{rel}]^T$. The antenna has been optimized for minimum reflection within the UWB frequency range (3.1 GHz to 10.6 GHz). The computational model is implemented in CST Microwave Studio and evaluated using its transient solver.

For both structures, ten algorithm runs have been executed with random initial designs. The results for the proposed algorithm are presented in Table I and compared to the results obtained with the reference TR algorithm. The following acceptance threshold values were used φ_0 = 0, 0.025, 0.05, 0.1, 0.2 and 0.3. The higher the threshold value, the lower the savings are, which is due to the more stringent condition for applying the Broyden update formula (and FD performed more frequently). The results for φ_0 = 0 (Broyden-only Jacobian updates) are enclosed in order to demonstrate that this version does not yield acceptable design quality. The frequency characteristics before and after optimization have been shown in Fig 4. The proposed combined algorithm delivers considerable reduction of the number of EM simulations needed to find the optimized solution even for the highest

value of the threshold $\varphi_0 = 0.3$ (around 48% for the coupler and around 57% for the antenna. The presented results also reveal an important advantage of the proposed algorithm, namely that the solution quality is stable, virtually independent of the acceptance threshold value apart from when $\varphi = 0$. This applies to both the objective function value (bandwidth BW in the case of the coupler and maximum in-band reflection S_{11} for the antenna) and the standard deviation of the respective objective functions. The latter is used as a measure of the results repeatability.

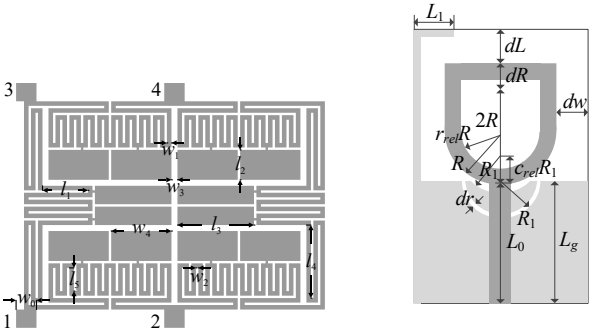

(a) (b)

Fig. 3. High-frequency structures used for verification of the proposed algorithm: (a) CMRC-based miniaturized microstrip rat-race coupler [37], and (b) wideband antenna [38].

Table I Performance Statistics of the Proposed Algorithm

Algorithm		Compact RRC				UWB Antenna			
		Cost[1]	Cost savings[2] [%]	BW[3] [GHz]	SD(B)[4] [GHz]	Cost[1]	Cost savings[2] [%]	Max $\|S_{11}\|$[5] [dB]	SD(max$\|S_{11}\|$)[6] [dB]
Reference		43.0	–	0.27	0.01	111.2	–	−14.9	0.6
φ_0	0[$]	15.9	63.0	0.17	0.12	27.4	75.4	−13.3	1.3
	0.025	17.4	59.5	0.19	0.10	31.0	72.1	−13.4	1.2
	0.05	20.3	52.8	0.22	0.10	35.5	68.1	−13.5	1.2
	0.1	22.0	48.8	0.19	0.11	43.0	61.3	−13.6	1.2
	0.2	22.6	47.4	0.20	0.11	51.1	54.0	−13.6	1.2
	0.3	22.4	47.9	0.20	0.11	47.4	57.1	−13.4	1.0

[1] Number of EM simulations averaged over 10 algorithm runs (random initial points);
[2] Percentage-wise cost savings w.r.t. the reference algorithm;
[3] Objective function values for the compact RRC (bandwidth BW in GHz);
[4] Standard deviation of BW in dB across 10 algorithm runs;
[5] Objective function values for the UWB antenna (maximum in-band reflection S_{11} in dB);
[6] Standard deviation of S_{11} in dB across 10 algorithm runs;
[$] Broyden-only Jacobian updates meaning no FD used whatsoever.

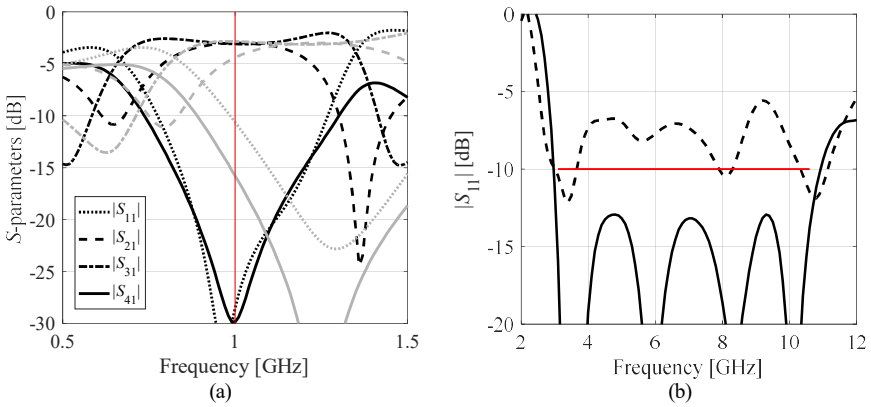

Fig. 4. Reflection characteristics of the considered high-frequency components for the representative algorithm runs: (a) compact RRC, (b) UWB antenna: initial and optimized design are marked gray and black, respectively. The vertical line in (a) indicates the required operating frequency f_0, whereas the horizontal line in (b) the design specifications.

Table II Performance Statistics of the Algorithm Utilizing Only BUP

Algorithm		Compact RRC				UWB Antenna			
		Cost[1]	Cost savings[2] [%]	BW[3] [GHz]	SD(B)[4] [GHz]	Cost[1]	Cost savings[2] [%]	Max $\|S_{11}\|$[5] [dB]	SD(max$\|S_{11}\|$)[6] [dB]
Reference		43.0	–	0.27	0.01	111.2	–	−14.9	0.6
φ_0	0[$]	15.9	63.0	0.18	0.11	26.5	76.2	−13.3	1.7
	0.025	13.4	68.8	0.20	0.06	37.5	66.3	−13.9	1.3
	0.05	28.9	32.8	0.23	0.04	47.9	56.9	−14.0	0.9
	0.1	27.0	37.2	0.22	0.05	58.4	47.5	−13.7	1.1
	0.2	42.6	0.9	0.22	0.05	75.9	31.7	−14.3	0.9
	0.3	41.3	4.0	0.21	0.06	89.3	19.7	−14.2	0.8

[1] Number of EM simulations averaged over 10 algorithm runs (random initial points);
[2] Percentage-wise cost savings w.r.t. the reference algorithm;
[3] Objective function values for the compact RRC (bandwidth BW in GHz);
[4] Standard deviation of BW in dB across 10 algorithm runs;
[5] Objective function values for the UWB antenna (maximum in-band reflection S_{11} in dB);
[6] Standard deviation of S_{11} in dB across 10 algorithm runs;
[$] Broyden-only Jacobian updates meaning no FD used whatsoever.

The most suitable threshold value for the RRC is $\varphi_0 = 0.05$: it delivers the best bandwidth and the smallest value of the bandwidth standard deviation, as well as cost savings of around 53%. As far as the UWB antenna is concerned, the value $\varphi_0 = 0.025$ seems to be most appropriate: it delivers savings as high as 72%, while both the design quality and its repeatability are degraded only slightly.

In order to provide more in-depth analysis of the results, a supplementary Table II is provided, in which the results obtained with the sole usage of Broyden update procedure (without the accelerated procedure) are shown. The results presented in Table II exhibit more pronounced dependence of the design quality on the acceptance threshold value when compared to the combined (AUP and BUP) algorithm (see Table I). As φ_0 increases, the better the quality of the solution is, as expressed by the objective function value and its standard deviation across ten algorithm runs. At the same time, the cost savings drop significantly (to as low as 4% for the RRC and to around 20% for the antenna). Thus, the introduction of the second, AUP procedure allowed for higher savings delivering similar design quality.

4 Conclusions

In the paper, a procedure for expedited design optimization of high-frequency structures has been proposed. Our methodology accelerates a standard trust-region gradient-based algorithm with numerical derivatives by development and incorporation of an adaptive scheme for updating the Jacobians of the system under design. The scheme combines the two main mechanisms, selective Broyden updates (governed by measuring the alignment between the latest direction of the design relocation and the coordinate system basis vectors), as well as relative design changes with respect to the trust region size in respective directions. The latter allows for discriminating variables for which the response sensitivities are stable across the design space, which is often the case of antennas and microwave components. As demonstrated using a wideband antenna and a miniaturized microstrip coupler, the proposed algorithm allows for considerable computational savings without compromising the design quality. Various design trade-offs controlled by user-defined algorithm parameters have been investigated as well. The algorithm can be used not only to expedite direct optimization of high-fidelity EM models, but also to speed up surrogate-assisted procedures involving variable-fidelity simulations. The future work will be focused on incorporating the proposed methodology into surrogate-based optimization frameworks.

Acknowledgement

The authors thank Dassault Systemes, France, for making CST Microwave Studio available. This work is partially supported by the Icelandic Centre for Research (RANNIS) Grant 174114051, and by National Science Centre of Poland Grant 2015/17/B/ST6/01857.

References

1. Koziel, S., Yang, X.S., Zhang, Q.J. (Eds.): Simulation-driven design optimization and modeling for microwave engineering, Imperial College Press, 2013.
2. Hao, Z.C., He, M., Fan, K., Luo, G.: A planar broadband antenna for the E-band gigabyte wireless communication. IEEE Trans. Ant. Prop., 65(3), 1369–1373, (2017).
3. Yao, Z., Wu, K., Tan, B.X., Wang, J., Li, Y., Zhang, Y., Poon, A.W.: Integrated silicon photonic microresonators: emerging technologies. IEEE J. Selected Topics in Quantum Electronics, 24(6), (2018).
4. Mailloux, R.J.: Phased array antenna handbook. 2nd ed. Artech House, Boston, 2005.
5. Simpson, D.J., Psychogiou, D.: Coupling matrix-based design of fully reconfigurable differential/balanced RF filters. IEEE Microwave Wireless Comp. Lett. 28(10), 888–890, (2018).
6. Bandler, J.W., Cheng, Q.S., Dakroury, S.A., Mohamed, A.S., Bakr, M.H., Madsen, K., Søndergaard, J.: Space mapping: the state of the art. IEEE Trans. Microwave Theory Tech., 52(1), 337–361, (2004).
7. Sevgi, L.: Electromagnetic modeling and simulation. IEEE Press Series on Electromagnetic Wave Theory, 2014.
8. Guo, D., He, K., Zhang, Y., Song, M.: A multiband dual-polarized omnidirectional antenna for indoor wireless communication. IEEE Ant. Wireless Prop. Lett., 16, 290–293, (2017).
9. Wen, D., Hao, Y., Munoz, M.O., Wang, H., Zhou, H.: A compact and low-profile MIMO antenna using a miniature circular high-impedance surface for wearable applications. IEEE Trans. Ant. Prop., 66(1), 96–104, (2018).
10. Wu, J., Sarabandi, K.: Compact omnidirectional circularly polarized antenna. IEEE Trans. Ant. Prop., 65(4), 1550–1557, (2017).
11. Ding, K., Gao, C., Qu, D., Yin, Q.: Compact broadband MIMO antenna with parasitic strips. IEEE Ant. Wireless Prop. Lett., 16, 2349-2353, (2017).
12. Shao, W., He, J., Wang, B.-Z.: Compact rat-race ring coupler with capacitor loading. Microwave and Optical Technology Letters. 52 (1), pp. 7–9, (2010).
13. Tseng, C.-H., Chang, C.-L.: A rigorous design methodology for compact planar branch-line and Rat-Race couplers with asymmetrical T-structures. IEEE Transactions on Microwave Theory and Techniques. 60(7), 2085–2092, (2012).
14. Wang, J., Wang, B.-Z., Guo, Y.X., Ong, L.C., Xiao, S.: Compact slow-wave microstrip rat-race ring coupler. Electronics Letters. 43(2), pp.111–113, (2007).
15. Verma, S., Rano, D., Hashmi, M.S.: A novel miniaturized band stop filter using fractal type defected ground structure (DSG). IEEE Asia Pacific Microwave Conference(APMC), 799–802, (2017).
16. Haq, M.A., Koziel, S., Cheng, Q.S.: Miniaturization of wideband antennas by means of feed line topology alterations. IET Microwaves Ant. Prop., 12(3), 2128–2134, (2018).
17. Vendik, I.B., Rusakov, A., Kanjanasit, K., Hong, J., Filonov, D.: Ultrawideband (UWB) planar antenna with single-, dual- and triple-band notched characteristic based on electric ring resonator. IEEE Ant. Wireless Prop. Lett., 16, 1597–1600, (2017).
18. Conn, A.R., Gould, N.I.M., Toint, P.L.: Trust Region Methods, MPS-SIAM Series on Optimization, 2000.

19. Lalbakhsh, A., Afzal, M.U., Esselle, K.P.: Multiobjective particle swarm optimization to design a time-delay equalizer metasurface for an electromagnetic band-gap resonator antenna. IEEE Ant. Wireless Prop. Lett., 16, 915–915, (2017).
20. Ullah, U., Koziel, S.: A broadband circularly polarized wide-slot antenna with a miniaturized footprint. IEEE Ant. Wireless Prop. Lett., 2018.
21. Liu, Y.Y., Tu, Z.H.: Compact differential band-notched stepped-slot UWB-MIMO antenna with common-model suppression. IEEE Ant. Wireless Prop. Lett., 16, 593-596, (2017).
22. Koziel, S., Bekasiewicz, A.: Rapid design optimization of antennas using variable-fidelity EM models and adjoint sensitivities. Eng. Comp., 33(7), 2007–2018, (2016).
23. Xiao, L.Y., Shao, W., Ding, X., Wang, B.Z.: Dynamic adjustment kernel extreme learning machine for microwave component design. IEEE Trans. Microwave Theory Techn., 66(10), 4452–4461, (2018).
24. Koziel, S., Ogurtsov, S.: Antenna design by simulation-driven optimization. Surrogate-based approach. Springer, New York, 2014.
25. Koziel, S., Bekasiewicz, A.: Rapid microwave design optimization using adaptive response scaling. IEEE Transactions on Microwave Theory and Techniques. 64(9), 2749–2757, (2016).
26. Zhang, J., Zhang, C., Feng, F., Zhang, W., Ma, J., Zhang, Q.J.: Polynomial chaos-based approach to yield-driven EM optimization. IEEE Trans. Microwave Theory Techn., 66(7), 3186–3199, (2018).
27. De Villiers, D.I.L., Couckuyt, I., Dhaene T.: Multi-objective optimization of reflector antennas using kriging and probability of improvement. Int. Symp. Ant. Prop., 985–986, San Diego, USA, (2017).
28. Jacobs, J.P.: Characterization by Gaussian processes of finite substrate size effects on gain patterns of microstrip antennas. IET Microwaves Ant. Prop., 10(11), 1189–1195, (2016).
29. Easum, J.A., Nagar, J., Werner, D.H.: Multi-objective surrogate-assisted optimization applied to patch antenna design. Int. Symp. Ant. Prop., 339–340, San Diego, USA, (2017).
30. Zhu, J., Bandler, J.W., Nikolova, N.K., Koziel, S.: Antenna optimization through space mapping. IEEE Trans. Ant. Prop., 55(3), 651–658, (2007).
31. Koziel, S., Leifsson, L.: Simulation-driven design by knowledge-based response correction techniques. Springer, New York, 2016.
32. Koziel, S.: Fast simulation-driven antenna design using response-feature surrogates. Int. J. RF & Microwave CAE, 25(5), 394–402, (2015).
33. Koziel, S., Bekasiewicz, A.: Multi-objective design of antennas using surrogate models. World Scientific, 2016.
34. Koziel, S., Kurgan. P.: Compact cell topology selection for size-reduction-oriented design of microstrip rat-race couplers. Int. J. RF & Microwave CAE, 28(5), (2018).
35. Koziel, S., Kurgan. P.: Inverse modeling for fast design optimization of small-size rat-race couplers incorporating compact cells. Int. J. RF & Microwave CAE, 28(5), (2018).
36. Nocedal, J., Wright, S.J.: Numerical Optimization, 2nd edition, Springer, 2006.
37. Koziel, S., Bekasiewicz, A., Kurgan, P.: Rapid design and size reduction of microwave couplers using variable-fidelity EM-driven optimization, Int. J. RF & Microwave CAE, 26(1), 27-35, (2016).
38. Alsath, M.G.N., Kanagasabai, M.: Compact UWB monopole antenna for automotive communications, IEEE Trans. Ant. Prop., 63(9), 4204-4208, (2015).